Available online at www.sciencedirect.com
ScienceDirect
Journal of the European Ceramic Society 30 (2010) 2049–2055
www.elsevier.com/locate/jeurceramsoc

Fabrication of bioceramic scaffolds with ordered pore structure by inverse replication of assembled particles

Kenta Takagi [a,*], Takefumi Takahashi [b], Keiko Kikuchi [b], Akira Kawasaki [b]

[a] *Materials Research Institute for Sustainable Development, Advanced Industrial Science and Technology (AIST), Nagoya, 463-8560, Japan*
[b] *Department of Materials Processing, Graduate School of Engineering, Tohoku University, Sendai 980-8579, Japan*

Received 19 November 2009; received in revised form 8 March 2010; accepted 2 April 2010
Available online 5 May 2010

Abstract

β-Tricalcium phosphate (β-TCP) scaffolds with an ordered pore structure were fabricated by ceramic slip casting using a particle-assembled template. An ordered pore structure is expected to enable uniform and accurate improvement in the topology of the porous structure of scaffolds. Monosized spherical polyethylene particles were self-assembled into an fcc lattice by close-packing with a pyramidal indentation and heat-treated for interparticle necking. β-TCP slurry was cast with this particle array, followed by heat treatments to burn out the particles and sinter the β-TCP frame. The sintered scaffold showed not only an ordered arrangement of uniform pores but also pore interconnection pathways, which faithfully replicated the particle-assembled structure. High porosity, high pore interconnectivity, and structural controllability, as well as high accessibility, were achieved by this process.

Keywords: Particle self-assembly; Slip casting; Porosity; Biomedical applications

1. Introduction

In recent years, bioceramic scaffolds have generated great interest in the field of tissue engineering, e.g. for bone regeneration.[1] A scaffold is used to fill in a bone cavity formed by trauma or tumour removal, and it serves as a template for the migration and proliferation of cells and vessels that are necessary for bone regeneration.[2] Thus, a scaffold is generally required to have a bimodal porous structure comprising interconnected macropores and micropores. The interconnected macropores act as channels for the transport of bodily fluids, vessels and cells such as osteoclasts and osteoblasts. These invading cells attach to the surfaces of macropores, and gradually substitute autologous bone for the synthetic scaffold by bioreactions. A continuous structure of micropores facilitates the attachment of cells and the excretion of metabolic waste.[3]

Recent researches are bringing out more detailed geometric criteria of pore structure for efficient bone substitution. Macropores must be larger than 100 μm for enabling the invasion of cells,[4] and high macropore porosity is preferred for increasing the number of cells for attachment.[5] The interconnection pathway of macropores is the most important criterion. The macropores ought to be well connected by the interconnection pathways, with an adequate size to circulate the body fluids that transport osteogenetic cells and nutriments. Lu et al. reported that interconnection pathways larger than 50 μm are necessary for osteogenesis.[6]

In order to fabricate an effective bioscaffold, further improvement in the topology of the pore structure, as well as satisfaction of the abovementioned criteria, is required. To date, conventional ceramic foaming methods and pore-forming agent methods have been used to fabricate a number of scaffolds; interconnected pore structures and high porosity have been achieved by these methods.[7–11] However, these methods provide limited control over the pore structure to implement topological improvements, because the conventional scaffolds comprise a random pore structure. From this point of view, rapid prototyping methods have recently been used in an attempt to fabricate scaffolds with a controlled pore network.[12–15] The limited control of a random pore structure is attributed to the elusive positional relationship between the pores; thus, an ordered pore structure might enable the uniform control of the pore size and interconnections.

* Corresponding author. Tel.: +81 52 736 7203; fax: +81 52 736 7406.
E-mail address: k-takagi@aist.go.jp (K. Takagi).

0955-2219/$ – see front matter © 2010 Elsevier Ltd. All rights reserved.
doi:10.1016/j.jeurceramsoc.2010.04.009

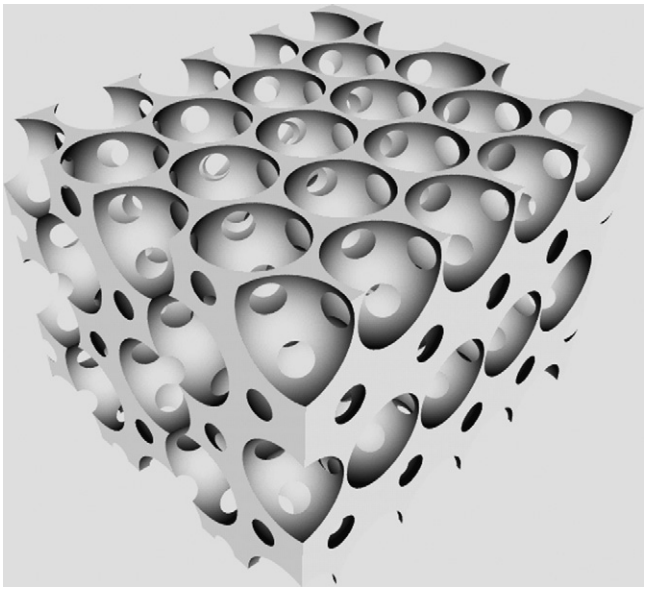

Fig. 1. Schematic structure of an ordered pore bioscaffold with uniform interconnections.

Therefore, we are interested in a scaffold with an ordered pore structure. One way to achieve such a structure would be to adopt a method similar to that used in our research on photonic band-gap structures, i.e. a replication method using a particle-assembled template.[16] This approach allows to produce a porous structure having interconnected spherical pores with an fcc structure, as shown in Fig. 1. In the case of scaffolds, the right method for replication would be to use ceramic slurry casting. The geometry of the pores and their interconnection pathways should be identical to that of the particles and interparticle necks formed in the particle-assembled template. Adjustments to the particle size and interconnections are thus expected to enable the direct control of the macroporous structure of the resulting scaffold. Moreover, ordered structures of spherical pores are expected to have advantages over the other structures in mechanical properties. For example, the three-dimensionally (3D) periodic structures of spherical pores have been predicted to possess a high elastic property with anisotropy.[17] The proposed process is likely to be uncomplicated and accessible because it does not require special instruments.

The aim of this study was to fabricate bioscaffolds with an ordered pore structure by a combination of particle self-assembling and ceramic slurry casting. As the first step toward the advanced scaffolds, we mainly discussed about the practicability of fabrication of these scaffolds and the controllability of the pore structure in the present study. Thus, the fabricated samples were characterized in terms of their pore structure, particularly their macropore interconnections.

2. Experimental procedures

2.1. Preparation of monosized particles and templates

Scaffolds were formed in four steps: preparing monosized spherical particles, self-assembling the particles to form templates, casting bioceramic slurry into the templates, and sintering. First, monosized spherical particles were prepared using polyethylene (PE) for forming casting templates; PE was chosen because it is a well-known pyrolytic material. Commercially available low-density PE (HW2203A, Mitsui Chemical Co. Ltd., Japan) was melted at 413 K and mixed with 10 vol% carbon powder (99.9% purity, average particle size: 5 μm) to form an ingot. The carbon powder was added both to blacken the PE ingot and increase its density for subsequent spheroidization. After defoaming and solidifying, the PE ingot was mechanically pulverized into a powder with a grain size of the order hundreds of micrometers. The obtained grains were dropped in hot silicone oil placed in a 500-mm-long tube. The upper half of the silicone oil was heated up to 413 K, while the bottom half was maintained at room temperature. The melted grains in the hot region spontaneously formed spherical shapes by surface tension, and then, they were solidified during falling in the cool region. The obtained spherical particles were adequately soaked in hexane to remove the silicone oil. At this stage, the as-received particles were fairly polydispersed. Then, they were precisely classified by size into various types of monodispersed particles using a twin-roll classification method: particles with the desired size were selected by passing through a definite opening between two cylinders. In the present study, monosized particles with sizes ranging from 300 to 600 μm were prepared. The size distributions of the prepared particles were evaluated using an optical microscope coupled with an image analyzer.

Interparticle necks were formed in the particle-assembled templates by thermal joining. As described earlier, the size of these interparticle necks directly determine the size of the pore interconnection pathways in the resulting scaffolds. Thus, understanding the necking behaviour is indispensable for controlling the structure of pore interconnections. The interparticle thermal joining was carried out using a one-dimensional particle array, prior to 3D assembling. Five of the prepared particles were aligned, touching each other, on a wedge-shaped stage whose sides were inclined at an angle of 45°. The particles on the stage were heated in an oven for 1 h at temperatures ranging from 368 to 378 K. The joined particles were characterized using a scanning electron microscope (SEM) and the image analyzer.

Next, 3D templates were prepared by the self-assembly method. Monosized spheres confined in a pyramidal space are naturally close-packed into an fcc structure by gravity and vibration.[16] Thus, an indentation with the shape of an equilateral quadrangular pyramid was made from brass. This indentation was filled with monosized PE particles and adequately vibrated. To form interparticle necks, the assembled particles in the indentation were heated for 1 h at the temperature that was optimized during the pre-examination. The sizes of the interparticle necks in some arrays were measured using the SEM while the arrays were gradually disassembled from outside.

2.2. Preparation of β-TCP slurries

Meanwhile, bioceramic slurries were prepared for forming the frames of scaffolds. β-Tricalcium phosphate (β-TCP) was chosen as the scaffold material because of its excellent

bioresorbability. Two types of β-TCP powders with different particle sizes were used as the raw material to obtain the desired microstructure. As-received commercial β-TCP powder with an average particle size of 5 μm (Aldrich, USA) was used as a coarse powder. A fine powder was obtained from the coarse powder by wet ball milling using ethanol medium and zirconia pot and balls; the resulting particle size was 1.5 μm. Each powder was adequately dispersed in water containing polyvinyl alcohol as a binder and polyester acrylate copolymer as a dispersant, by ultrasonication. The mixing ratio of the powder, binder, dispersant, and water was fixed at 42.63:0.65:0.81:55.91 (in vol%). The viscosities of the obtained slurries were measured using a rotational viscometer (RM180, Rheometeric Scientific, USA).

2.3. Fabrication of periodic microporous scaffolds

Before fabricating the scaffolds, the prepared slurries were sintered at various temperatures without the templates to investigate their sintering behaviour. The slurry was poured into a cylindrical mold with a diameter of 13 mm, and then, it was slowly dried in air. The preforms were gently heated in air up to 732 K at a heating rate of 0.2 K min^{-1} to burn out the slurry additives. The heating conditions were determined from a thermogravimetric analysis of the additives. Subsequently, the samples were sintered in air at temperatures ranging from 1173 to 1573 K.

Finally, scaffolds were fabricated using the prepared templates and β-TCP slurry. The templates were immersed in the slurry placed in the mold. The samples were placed in a low pressure atmosphere to completely infiltrate the slurry into the internal space of the templates. The samples were dried in air and then machined to expose all the outermost particles of the embedded templates. To burn out the slurry additives, the preforms were heated in the same manner as the bulk samples. Subsequently, the samples were heated up to 1173 K at 1 K min^{-1} to burn out the template composed of PE and carbon. Finally, the samples were sintered at 1473 K for 2 h in air.

The densities of the sintered bulk samples were measured by the Archimedes method. Phase identification and microstructural characterization of the samples were performed using an X-ray diffractometer and the SEM coupled with the image analyzer. In particular, the interconnection pathways in the scaffolds were observed individually as the scaffolds were gradually ground.

3. Results and discussion

The combination of the particle self-assembling and slip casting processes was used to fabricate bioscaffolds with an ordered pore structure. The periodic structure of the particle-assembled templates was replicated in the resulting scaffolds by this method. Hence, the first touchstone for the successful application of this process was the fabrication of the particle-assembled templates. In addition, the geometric controllability of the templates had to be demonstrated. Therefore, an interparticle necking test was conducted prior to the fabrication of the templates. For this test, monosized PE particles with four different diameters (300, 400, 500, and 600 μm) were prepared. All the particles showed a perfect spherical shape and very smooth surface with no voids generated by solidification shrinkage, as shown in Fig. 2. These were beneficial for the formation of necks with uniform sizes.

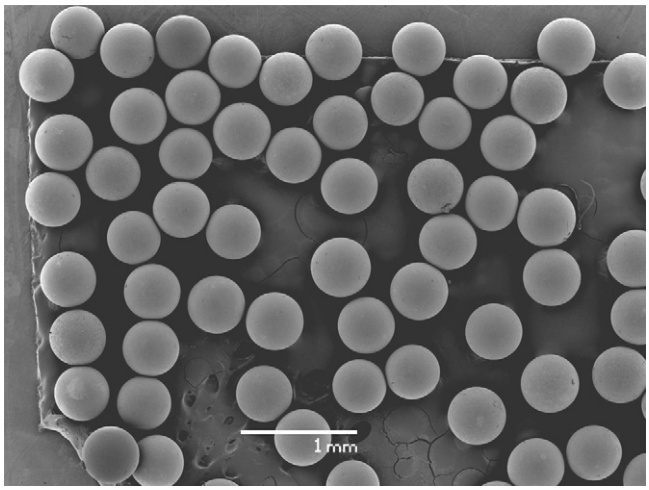

Fig. 2. SEM micrograph of the prepared monosized spherical PE particles with a diameter of 500 mm.

The prepared particles were one-dimensionally aligned and thermally joined at various temperatures. The joining temperatures were set below PE's melting point (380 K) to prevent the distortion of the particles. The heat treatments resulted in the formation of strong necks between the particles, as shown in Fig. 3(a). The necks showed a very symmetrical concave shape like a typical sintered neck (Fig. 3(b)). These necks were supposed to be formed by viscous flow deformation driven by

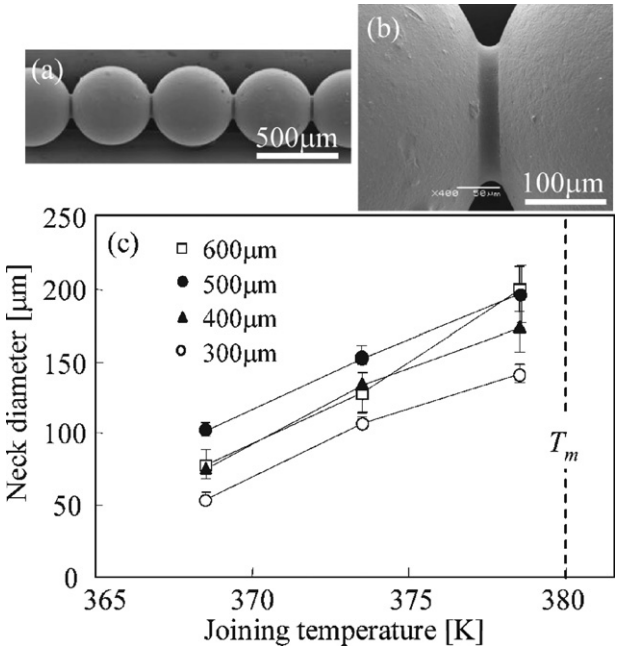

Fig. 3. Interparticle necking of one-dimensionally arrayed PE particles by thermal joining. (a) Overview of 500-mm particles after joining at 373 K. (b) SEM photo of a joined region in the array shown in (a). (c) Changes in neck diameters as a function of the joining temperature for particles with various diameters.

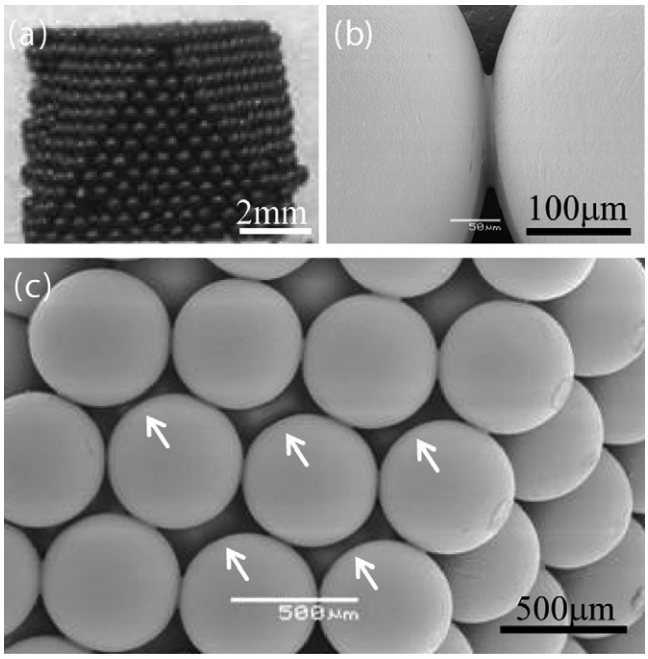

Fig. 4. Template fabricated by particle self-assembly and interparticle joining. (a) Optical photo of the template. (b) SEM photo of a joined region in the template. (c) SEM photo of the outermost layer. Arrows indicate unconnected sites.

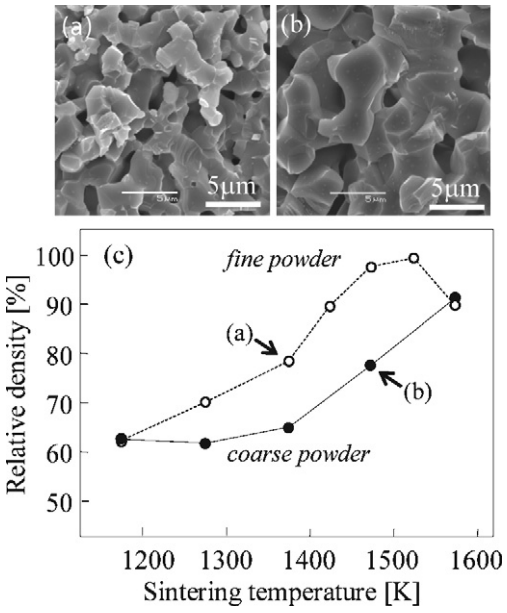

Fig. 5. Sintering behaviours of the coarse (5 mm) and fine (1.5 mm) β-TCP powders. (a and b) SEM fractographs of the samples sintered from the fine powder at 1373 K and from the coarse powder at 1473 K. (c) Relationship between the sintering temperature and sintered density.

surface tension, rather than by diffusion as in sintering. Despite the non-diffusive bonding, no boundaries or voids were observed in the formed necks. In addition, the neck diameters were almost uniform in a single array and increased linearly with increasing the joining temperature, as shown in Fig. 3(c). Increasing the joining temperature led to a decrease in the viscosity of PE, resulting in an increase in the neck diameter. This result suggests that the sizes of the interparticle necks in a template can be simply controlled all at once by the joining temperature. In addition, the neck diameters obtained in this study ranged from 50 to 200 μm, which fulfilled the criteria for pore interconnection size in a scaffold (>50 μm).

Subsequently, the particle-assembled templates were fabricated by self-assembling and interparticle joining. We used monosized PE particles with an average size of 566 μm and a size dispersion of 6.6% in standard deviation units: the particle sizes ranged from 540 to 600 μm. The joining temperature was set at 373 K, which was expected to enable the formation of necks with a diameter of about 150 μm, according to the result of the 1D joining test. The particle-ordered structure with the fcc lattice was successfully fabricated by this process, as shown in Fig. 4(a). The arrays could be quickly formed without the need for special skill by using this self-assembling method. The heat-treated arrays were robust enough for direct handling owing to the strong necking. Fig. 4(b) shows the outermost layer of the array, which corresponds to the (1 1 1) face of the fcc lattice. Most of the particles were connected to the nearest particles via the necks, similar to the 1D arrays. However, a number of non-connected points were found at sites where an ideal fcc packing would have made a connection, as indicated by the arrows in Fig. 4(c). These connection failures may have been caused by disordering of the periodicity owing to the relatively high size dispersity of the particles used, which is common in particle self-assembly.[18,19] This problem will be quantitatively discussed in a later section, because it is closely related to the pore interconnectivity of the resulting scaffolds.

Meanwhile, to provide a scaffold frame with an appropriate micropore structure, the sintering behaviour of the prepared β-TCP slurries was preliminarily examined using cylindrical bulk samples without the templates. In the present study, two types of powders with the different sizes of 5 μm (coarse) and 1.5 μm (fine) were used to investigate the controllability of sintered microstructure. As for the preparation of slurries, we chose the low powder loading of 43 vol% compared to common ceramic slurries. This was because their moldability to the intricate templates should be taken account rather than sintering densification for the fabrication of scaffolds. Indeed, the prepared slurries composed of the coarse and fine powders were confirmed to have the low viscosities of 35 and 30 mPa s at a share rate of 100 s^{-1}, respectively. Fig. 5(c) shows the relationships between the sintering temperature and relative density for the two types of slurries. The density of the sintered β-TCP could be conveniently controlled over a wide range more than 60% by adjusting the sintering temperature and powder size. In the case of the fine powder, the sintered density reached to high value larger than 95% despite of the low powder loading. It, however, dropped above 1573 K. This was attributed to the well-known phase transformation from β- to α-TCP,[20] in which the density of TCP decreases from 3.07 to 2.86 g/cm.[3,21] Indeed, a small amount of the α-TCP phase was detected in the X-ray diffraction results of the samples sintered at 1573 K. It was feared that the β-to-α transformation might lead to some harmful effects on the functions of the scaffolds: α-TCP shows less bio-absorbability than β-TCP.[22] In addition, the precipitation

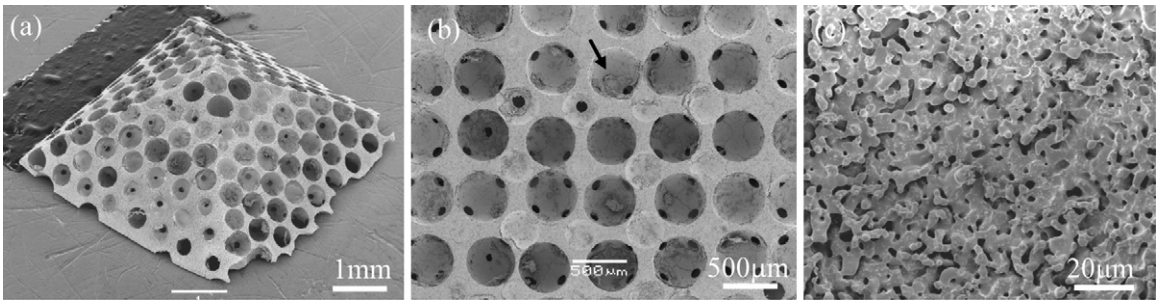

Fig. 6. SEM photos of the fabricated scaffold. (a) Overview and (b) cross section of the (1 1 1) face of the scaffold. The arrow indicates a delamination. (c) Surface of a macropore.

of α-TCP might cause a decline in the strength of the sintered body because the volume shrinkage during transformation generates internal stress. Actually, the results of a diametral tensile strength (DTS) test[23] verified that the strength steeply declined by about 30% (from 45 to 13 MPa) with an increase in the sintering temperature from 1473 to 1523 K. This result also implied that the actual precipitation temperature of the α-TCP phase was around 1523 K, rather than 1573 K. On the other hand, both the powders formed the network structures of the micropores with the sizes corresponding to the respective powder sizes, as observed from Fig. 5(a) and (b). These sizes covered the sizes of the micropores that have been reported effective in promoting bone ingrowth (2–5 μm).[24–26] Consequently, the prepared β-TCP slurries were a promising cast material for constructing the scaffold frame with the suitable microporous structure.

Finally, the fabrication of scaffold was carried out using the slurry and the template assembled from 566-μm particles with a size distribution of 6.6%. In this study, the slurry with the coarse β-TCP powder was adopted, because both the types of the slurries had almost the same low-viscosity and provided the high microporosities in a similar manner. The preform prepared by the slip casting was heat-treated to burn out the organic additives and template. At this point, it was confirmed by X-ray diffraction that the heat-treated sample included no product that was generated by a reaction between β-TCP, carbon, and PE. This sample was subsequently sintered at 1473 K. The produced scaffold maintained the original shape of the preform, as shown in Fig. 6(a). As expected, the interior of the scaffold was comprised of the macroporous ordered structure (Fig. 6(b)). The internal macropores showed a nearly spherical shape with many interconnection pathways. Although it was very difficult to determine the exact diameters of the macropores from two-dimensional observations, the SEM images showed that the diameters were approximately 500 μm. Moreover, the observation found no noticeable defects such as distortion and cracking but some pore surface delaminations, as indicated by the arrow. These delaminations were produced by the lamellar aggregation of the powder owing to the meniscus of molten PE during the heat treatment. However, these thin delaminations will supposedly show little effect on the functions of the scaffold. The scaffold frame was comprised of properly interconnected micropores, as shown in Fig. 6(c). This microporous structure was similar to that of the bulk samples in Fig. 5(b). Image analysis was carried out for SEM images of polished cross-sections of the scaffold and bulk samples sintered at the same temperature to compare their microporosities. The measured porosity of the scaffold was 24.4%, which was a little smaller than that of the bulk sample, 26.9%. The additional densification in the scaffold frame would occur by powder rearrangement promoted by the molten PE during the heat treatment as mentioned above. However, this slight difference between the scaffold and bulk samples would not matter for controlling the micropore structure. As a result, the geometry of the template appeared to be faithfully transferred to the resulting scaffold despite shrinkage. Thus, the macroporosity in the fabricated scaffold should almost coincide with the filling ratio of fcc lattice, i.e. 76%. From the macroporosity and the measured microporosity, the total porosity was calculated to be 82%, which was equivalent to the scaffolds that have been ever fabricated by the other pore-forming agent methods.[27]

In this study, we particularly focused on the interconnection of macropores, because it cannot be controlled in the conventional random pore structures. As shown in Fig. 5(b), a number of interconnection pathways were formed in the macropores, and their sizes appeared to be almost uniform. This uniformity is one of the great benefits of an ordered pore structure. On the other hand, all the interconnections were located at specific sites representing contact points in the fcc lattice. However, some vacant connection sites were also found, that is, interconnection failures. These failures definitely originated from the interparticle necking failures that occurred during the particle self-assembling process, as described earlier.

Fig. 7 shows the size distributions of the necks and interconnections, which were measured as the template and scaffold

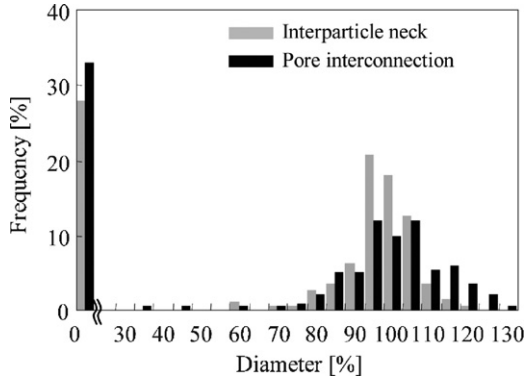

Fig. 7. Size distributions of the interparticle necks and pore interconnections. Zero represents the necking or pore interconnection failures.

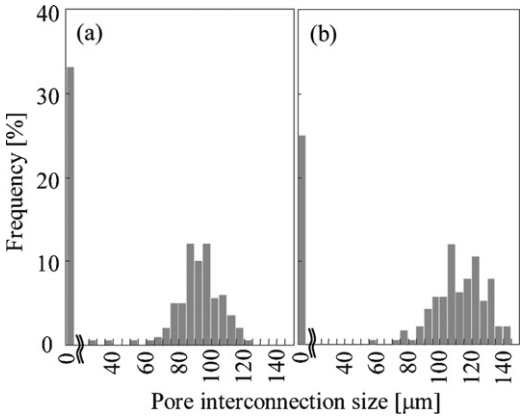

Fig. 8. Comparison of the size distributions of macropore interconnections between the two scaffolds fabricated from the PE particles with size distributions of (a) 6.6% and (b) 4.2%.

were gradually broken. Note that zero on the lateral axis in this histogram represents the necking or interconnection failures. The diameters of the interconnections in the scaffold were distributed in a narrow range of 80–130 μm. Conventional scaffolds with random pore structures have been reported to show a very wide size distribution, for example, from several tens to hundreds of micrometers.[28] As compared to these, the interconnection size of the present sample might be considered to be very uniform. Moreover, the important point was the controllability of the interconnection size. By seeing Fig. 7, the size distributions of the interconnections agreed with those of the necks, except a few minor differences. The average interconnection size (98 μm) was also in good agreement with the average neck size (95 μm). In other words, the necks in the template were transferred to the scaffold as interconnection pathways. The size of the necks formed between the PE particles in the template has been already demonstrated to be easily controllable by the interparticle joining conditions. Thus, the sizes of the macropore interconnection in the scaffold can be uniformly controlled by adjusting the joining temperature. Further, Fig. 7 indicates that interconnections were formed in 67% of the contact points in an ideal fcc lattice. As the coordination number of an ideal fcc lattice is 12, the interconnectivity (ratio between the number of interconnections per volume and the numbers of pores per volume) in the fabricated scaffold was calculated to be 8.0. This value was larger than the values obtained from conventional random pore scaffolds, for example, connectivity of 2.1 reported by Bohner et al.[10] This high connectivity ensured the non-existence of isolated macropores.

On the other hand, the interconnection failure of 33% was originated from the disordering of periodicity in the particle-assembled template owing to the polydispersion of raw PE particles. In our previous research, we showed that a reduction in the polydispersity of constituent particles improves the periodicity of the resulting array.[19] Hence, another scaffold was fabricated using PE particles with a size of 567 μm and a higher monodispersity of 4.2%. Fig. 8 shows a comparison between the size distributions of the interconnections between the two scaffolds derived from the PE particles with the different size dispersities. As predicted, the reduction in the polydispersity resulted in a decrease in the pore interconnection failures by nearly 10%. Moreover, with reducing the polydispersity of particles, the size distribution of the interconnections was shifted to a larger value, and the average size increased to 118 μm, which was closer to the expected size of 150 μm. This reason could be explained as follows: an imperfect close-packing generated non-uniformity in the contact forces between the particles in the entire template. In this case, it is presumed that contact points with large force preferentially form a neck, while the other contact points are not provided with sufficient force. Thus, the enhancement of monodispersity led to more uniform and sufficient contact forces, resulting in the interconnection sizes close to the expectation. As a result, the use of more monodispersed particles allowed both higher interconnectivity and more accurate controllability of the interconnection size in the scaffold. Lately, new atomization processes capable of mass-producing precise monosized particles of various materials have been developed in the field of powder metallurgical engineering.[29,30] Highly monosized particles produced by such an advanced atomization process should allow excellent controllability of interconnection size as well as improvement of interconnectivity.

The results of this study suggested that the replication method with the particle-assembled template and slip casting is capable of controlling the size and interconnection size of macropores, and the size and the porosity of the micropores in the scaffolds. As for the macroporosity, the present method can provide only 76% which is the filling ratio of fcc lattice. It is quite possible that the macroporosity may be adjusted by an additional process: for example, densifying of the template by an isostatic pressing, and thinning of the PE spheres in the template by chemically dissolving. On the other hand, a bioscaffold requires mechanical properties such as the strength and stiffness, as well as the improvement of porous structure. Maldovan et al. have reported that porous materials composed of spherical pores arranged on the fcc lattice points have high elastic moduli, particularly on the ⟨1 1 1⟩ direction.[17] Therefore, the obtained scaffolds are expected to exhibit higher elastic properties than the conventional scaffolds with the random and rod-connected porous structures. Strength of scaffolds with the multi-scale porosity is supposed to be primarily determined by the macroporosity, microporosity and micropore size. Also stress concentration around the interconnections must influence on the strength. Thus, design of these geometrical parameters in terms of strength is also needed. Further research on the mechanical properties of the scaffold produced by the suggested method is underway.

4. Conclusion

β-TCP bioscaffolds with an ordered porous structure were fabricated by a combination of particle self-assembling and ceramic slip casting. Templates with an fcc structure of monosized polyethylene particles were prepared by particle self-assembling and thermal interparticle necking processes. β-TCP slurry was infiltrated into the particle-assembled template, followed by heat treatments to burn out the particles and sinter

β-TCP. The fabricated scaffold showed an ordered pore structure with uniformly sized macropores and pore interconnection pathways that faithfully replicated the particles and their necks in the template, respectively. In addition, the fcc structure of the macropores led to high porosity and high macropore interconnectivity. The interconnectivity could be improved by the use of highly monosized particles. On the other hand, the diameter of the interparticle necks was demonstrated to be easily varied by the necking temperature. Therefore, the size of the pore interconnections in the resulting scaffold could be controlled uniformly. As a result, the use of an ordered pore structure was shown to be effective in controlling the macropore structure for improving the topology of ceramic bioscaffolds.

References

1. Karageorgiou V, Kaplan D. Porosity of 3D biomaterial scaffolds and osteogenesis. *Biomaterials* 2005;**26**:5474–91.
2. Shiratori K, Matsuzaka K, Koike Y, Murakami S, Shimono M, Inoue T. Bone formation in b-tricalcium phosphate-filled bone defects of the rat femur: morphometric analysis and expression of bone related protein mRNA. *Biomed Res* 2005;**26**:51–9.
3. Lampin M, Warocquier-Clerout R, Legris C, Degrange M, Sigot-Luizared MF. Correlation between substratum roughness and wettability, cell adhesion, and cell migration. *J Biomed Mater Res* 1997;**36**:99–108.
4. Hulbert SF, Morrison SJ, Klawitter JJ. Compatibility of porous ceramics with soft tissue: application to tracheal prostheses. *J Biomed Mater Res* 1971;**5**:269–79.
5. Gauthier O, Bouler J-M, Aguado E, Pilet P, Daculsi G. Macroporous biphasic calcium phosphate ceramics: influence of macropore diameter and macroporosity percentage on bone ingrowth. *Biomaterials* 1998;**19**:133–9.
6. Lu JX, Flautre B, Anselme K, Hardouin P, Gallure A, Descamps M, et al. Role of interconnections in porous bioceramics on bone recolonization *in vitro* and *in vivo*. *J Mater Sci Mater Med* 1999;**10**:111–20.
7. Lemos AF, Ferreira JMF. Porous bioactive calcium carbonate implants processed by starch consolidation. *Mater Sci Eng C* 2000;**11**:35–40.
8. Descamps M, Richart O, Hardouin P, Hornez JC, Leriche A. Synthesis of macroporous β-tricalcium phosphate with controlled porous architectural. *Ceram Int* 2008;**34**:1131–7.
9. Tamai N, Myoui A, Tomita T, Nakase T, Tanaka J, Ochi T, et al. Novel hydroxyapatite ceramics with an interconnective porous structure exhibit superior osteoconduction in vivo. *J Biomed Mater Res* 2001;**59**:110–7.
10. Bohner M, van Lenthe GH, Grünenfelder S, Hirsiger W, Evision R, Müller R. Synthesis and characterization of porous β-tericalcium phosphate blocks. *Biomaterials* 2005;**26**:6099–105.
11. Koç N, Timuçin M, Korkusuz F. Fabrication and characterization of porous tricalcium phosphate ceramics. *Ceram Int* 2004;**30**:205–11.
12. Bae C-J, Kim H-W, Koh Y-H, Kim H-E. Hydroxyapatite (HA) bone scaffolds with controlled macrochannel pores. *J Mater Sci Mater Med* 2006;**17**:517–21.
13. William JM, Adewunmi A, Schek RM, Flanagan CL, Krebsbash PH, Feinberg SE, et al. Bone tissue engineering using polycaprolactone scaffold fabricated via selective laser sintering. *Biomaterials* 2005;**26**:4817–5827.
14. Lee SH, Zhou WY, Wang M, Cheung WL, Ip WY. Selective laser sintering of poly(L-lactide) porous scaffolds for bone tissue engineering. *J Biomim Biomater Tissue Eng* 2008;**1**:81–9.
15. Jun I-K, Koh Y-H, Song J-H, Kim H-E. Fabrication and characterization of dual-channeled zirconia ceramics scaffold. *J Am Ceram Soc* 2006;**89**:2021–6.
16. Takagi K, Seno K, Kawasaki A. Fabrication of a three-dimensional terahertz photonic crystal using monosized spherical particles. *Appl Phys Lett* 2004;**85**:3681–3.
17. Maldovan M, Ullal CK, Jang J-H, Thomas EL. Sub-micrometer scale periodic cellular structures: microframes prepared by holographic interference lithography. *Adv Mater* 2007;**19**:3809–13.
18. Allard M, Sargent EH. Impact of polydispersity on light propagation in colloidal photonic crystals. *Appl Phys Lett* 2004;**85**:5887–9.
19. Takagi K, Kanno H, Kikuchi K, Kawsaki A. Effect of polydispersity on photonic band gap of terahertz photonic crystals Fabricated by particle assembly. *Jpn J Appl Phys* 2009;**48**:122001.
20. Mathew M, Schroeder LW, Dicken B, Brown WE. The crystal structure of α-$Ca_3(PO_4)_2$. *Acta Crystallogr B* 1977;**33**:1325–33.
21. Dorozhkin SV. Calcium orthophosphates. *J Mater Sci* 2007;**42**:1061–95.
22. Yuan H, De Bruijn JD, Li Y, Feng J, Yang Z, De Groot K, et al. Bone formation induced by calcium phosphate ceramics in soft of dogs: a comparative study between porous a-TCP and b-TCP. *J Mater Sci Mater Med* 2001;**12**:7–13.
23. Pittet C, Lemaître J. Mechanical characterization of brushite cements: a Mohr circles' approach. *J Biomed Mater Res* 2000;**53**:769–80.
24. Dellinger JG, Eurell JAC, Jamison RD. Bone response to 3D periodic hydroxyapatite scaffolds with and without tailored microporosity to deliver bone morphogentic protein 2. *J Biomed Mater Res* 2005;**76A**:366–76.
25. Hing KA, Annaz B, Saeed S, Revell PA, Buckland T. Microporosity enhances bioactivity of synthetic bone graft substitutes. *J Mater Sci Mater Med* 2005;**16**:467–75.
26. Woodard JR, Hilldore AJ, Lan SK, Park CJ, Morgan AW, Eurell JAC, et al. The mechanical properties and osteoconductivity of hydroxyapatite bone scaffolds with multi-scale porosity. *Biomaterials* 2007;**28**:45–54.
27. Chevalier E, Chulia D, Pouget C, Viana M. Fabrication of porous substrates: a review of processes using pore forming agent in the biomaterial field. *J Pharm Sci* 2008;**97**:1135–54.
28. Mastrogiacomo M, Scaglione S, Martinetti R, Dolcini L, Beltrame F, Cancedda R, et al. Role of scaffold internal structure on in vivo bone formation in macroporous calcium phosphate bioceramics. *Biomaterials* 2006;**27**:3230–7.
29. Henein H. Single fluid atomization through the application of impulses to a melt. *Mater Sci Eng A* 2002;**326**:92–100.
30. Takagi K, Masuda S, Suzuki H, Kawasaki A. Preparation of monosized copper micro particles by pulsated orifice ejection method. *Mater Trans* 2006;**47**:1380–5.